

Thermometric and chemical studies of fluid inclusions in sphalerite from Rhodope lead-zinc deposits: Shumachevski Dol – Gyudyurska (Madan District) and Kenan Dere (Laki District), Bulgaria

Nikolay B. Piperov¹, Paraskev Petrov², Stela Atanassova-Vladimirova³

¹ Institute of General and Inorganic Chemistry, Bulgarian Academy of Sciences, Acad. G. Bonchev Str., Bl. 11, 1113 Sofia, Bulgaria; e-mail: pipernik37@abv.bg

² Sofia University “St Kliment Ohridski”, Faculty of Geology and Geography, 15 Tsar Osvoboditel Blvd, 1504 Sofia, Bulgaria; e-mail: parp@gea.uni-sofia.bg

³ Institute of Physical Chemistry, Bulgarian Academy of Sciences, Acad. G. Bonchev Str., Bl. 11, 1113 Sofia, Bulgaria; e-mail: statanasova@ips.bas.bg

(Received: 19 December 2022; accepted in revised form: 31 March 2023)

Abstract. The objects of this study are fluid inclusions in sphalerite crystals or selected parts of them from two Central Rhodopean deposits: Shumachevski Dol – Gyudyurska (Madan District) and Kenan Dere (Laki District). A set of data for temperature of homogenization and total salinity are presented. The locations of coupled data in coordinates T_h vs total salinity reveal that the Kenan Dere sphalerite has been deposited from solutions of higher temperature (280–374 °C) and lower salinity (2–5 wt.% NaCl-eqv.). Conversely, the Shumachevski Dol and Gyudyurska sphalerites show lower $T_h = 200–230$ °C and somewhat higher salinity ($S = 6–12$ wt.% NaCl-eqv.). Furthermore, it is likely that both late Kenan Dere and Gyudyurska sphalerites were deposited at 30–50 °C lower temperatures than the earlier ones. Additionally, Decrepitation Inductively-Coupled-Plasma Atomic-Emission-Spectrometry was applied to determine the cations in the inclusion solute. The vacuum decrepitation was also used for liberating the volatiles (H_2O , CO_2) and analysing them by mass spectrometry. On that account, more detailed preliminary studies of the process of decrepitation were performed. However, the Zn-concentration in sphalerite-hosted fluid inclusions cannot be evaluated and the results from syngenetic quartz offer the only possibility for obtaining information about ore-element content. On the basis of a compilation of both present and previously published data, it can be concluded that the hydrothermal fluid under the Central Rhodope Dome was constituted *in situ* as a closed system at a depth of ~1 km, under nearly lithostatic pressure (~200 bars), $T \geq 350$ °C, and NaCl-dominated salt content ~10%. Under these conditions, a solution with a pH of ~4.0–4.5 contains ore elements (Fe, Zn, Pb) as soluble chlorido-complexes; for Zn, the total concentration may reach 1 wt.%. Sulphide-S compound under these conditions is H_2S . The sphalerite deposition follows a reverse path of the chemical reactions. The elevation of the hydrothermal fluid along the extensional dislocations results in boiling (*i.e.*, separation of CO_2) and cooling. The temperature decrease destabilizes the chlorido-complexes and leads to an increase in the Zn^{2+} activity. On the other hand, CO_2 loss enhances pH, and thus dissociates H_2S , yielding HS^- and S^{2-} ions, needed for sphalerite deposition.

Piperov, N., Petrov, P., Atanassova-Vladimirova, S. 2023. Thermometric and chemical studies of fluid inclusions in sphalerite from Rhodope lead-zinc deposits: Shumachevski Dol – Gyudyurska (Madan District) and Kenan Dere (Laki District), Bulgaria. *Geologica Balcanica* 52 (1), 49–63.

Keywords: fluid inclusions, sphalerite, thermometry, D-ICP-AES, Rhodope Pb-Zn deposits.

INTRODUCTION

This study is dedicated to the memory of our late lecturer Prof. Dr Jordanka Minčeva-Stefanova (1923–2007). It is a continuation of her work on

sphalerites from Bulgarian deposits, and more specifically their morphology and geochemistry (Minčeva-Stefanova, 1973, 1974, 1977; Minčeva-Stefanova and Veselinov, 1981; Minčeva-Stefanova *et al.*, 1978, 1983).

Minčeva-Stefanova and Veselinov (1981) first documented by SEM-images the inner sculpture of fluid inclusions in sphalerite crystals from the Kenan Dere deposit. Meanwhile, Krāsteva and Gadževa (1986) used a Kofler-type heating stage to measure the homogenization temperature (T_h) of fluid inclusions (>1500 determinations) in quartz (Qrz), sphalerite (Sph), fluorite and carbonates from the Madan ore district. For sphalerite, in particular, 234 T_h measurements in the range from 280 °C to 85 °C were registered, most often in the range of 220–150 °C.

Later, Bonev and Kouzmanov (2002) applied USGS thermostage at the University of Geneva to determine T_h of fluid inclusions in transparent sphalerite from the Madan ore district, including the Shumachevski Dol deposit. The late sphalerite generation studied by these authors is represented by clear and bounded light brown, yellow or green specimens of cleiophane type. A part of this material was used in our study (SHD4–7, see below). Bonev and Kouzmanov (2022) yielded information for $T_h = 220–200$ °C (for primary) and $T_h = 190–160$ °C for secondary inclusions. Based on the last ice crystal melting temperature (T_m), the authors evaluated the total salinity of inclusions at 5–6 wt.% NaCl-eqv. Optical microscopy and scanning electron microscopy (SEM) were used for detailed morphological and structural investigations. The vapour-gas bubbles in inclusions were prospected by a Raman microprobe. Carbon dioxide of high density ($\rho \approx 0.18$ g/cm³, *i.e.*, $\rho_{CO_2} = 0.00198$ g/cm³ at STP), which corresponds to a partial $P_{CO_2} \approx 100$ bar at $T = 20$ °C and ~ 180 bar at $T = 250$ °C, was found.

In the present study, a redetermination of some microthermometric measurements is undertaken, aiming to test our non-commercial technique. Decrepiation-inductively coupled plasma (D-ICP) spectrometry is capable to supply data on the cation content of the inclusion fluid; mass-spectrometry (MS) can help in analysing the gases evolved by thermodecrepiation in vacuum, especially for CO₂ determination. The data obtained by fluid inclusions study of sphalerite from two deposits may contribute to the better understanding of the geochemical environment of sphalerite deposition.

MATERIAL

Sphalerite samples and fluid inclusions

Sphalerites from Bulgarian deposits (Minčeva-Stefanova, 1973) are studied in this work in conjunction with their chemistry as mentioned above.

Variations in colour due to the different iron content, as a possible indicator of the growth stages (generations), are of special interest (Minčeva-Stefanova, 1977). This is the leading trend when samples representing different stages, earlier or later, are selected in the same location or even in the same crystal.

The sphalerite specimens were collected from two deposits: Shumachevski Dol – Gyudyurska (SHD + GYU), Madan District, and Kenan Dere (KED), Laki District (Minčeva-Stefanova, 1973). The first deposit was considered to reveal two events (locations) of a single hydrothermal system (Minčeva-Stefanova, 1973; Bonev, 1977). A brief description of the samples analysed is given below:

- SHD-1, SHD-2 (coarse crystals of green cleiophane, late (III generation)). The material of light-brown large crystals, late (III generation), from 650 m level (sp. 810, National Museum of Natural History, NMNH), labelled as SHD-3, was also analysed;

- another large banded sphalerite crystal, late (II generation), sp. 851, donated by I. Bonev (see Bonev and Kouzmanov, 2002) is divided in four samples: light-brown core (SHD-4); brown material of the banded intermediate zone (SHD-5); dark-brown pieces of the same zone (SHD-6); and SHD-7, which is a mix of SHD-5 and SHD-6;

- GYU-12 is a coarse black sphalerite (I generation) from metasomatic ore formation, out of the skarns of Gyudyurska (sp. 801); sample GYU-12a consists of light-brown crystals; (sp. 805 and 805a are vein samples of early and late generations, respectively);

- early (I generation) massive banded crystal yielded three samples: light-brown core (sp. 23-k 9, KED-8); later (II generation) dark-brown (KED-9) and brown material from the peripheral zone (KED-10).

Bonev and Kouzmanov (2002) described in details fluid inclusions in the sphalerite and cleiophane specimens from the Shumachevski Dol deposit, supplying a set of microphotographs of fluid inclusions, as well as SEM images of their inner sculpture. We also recognize the same morphological types of primary, pseudosecondary, and rarely secondary inclusions. Some representatives are shown in Fig. 1a–j and Fig. 2a–e.

METHODS, TECHNIQUES AND PROCEDURES

Thermometry

A few doubly polished slides of studied crystals were prepared for microscope observation, but only some of them yielded inclusions suitable for

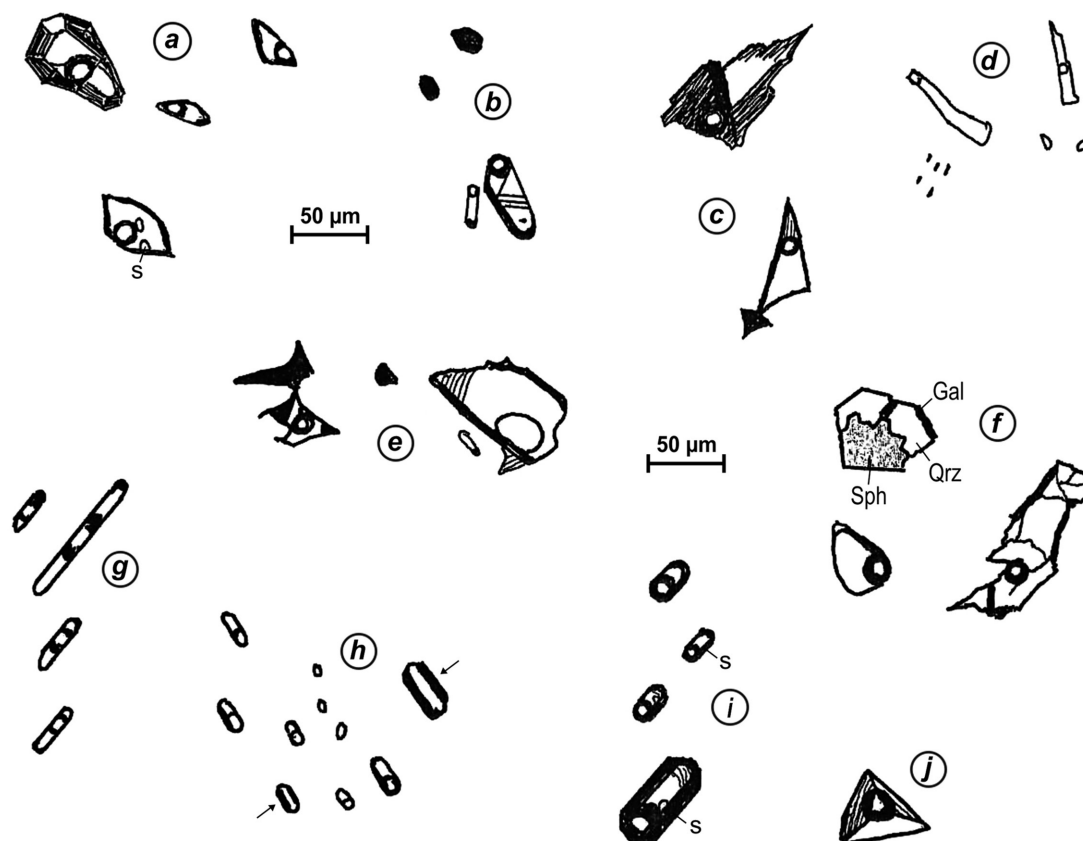


Fig. 1. Sphalerite-hosted fluid inclusions (the letters *P*, *PS* and *S* conform to their assumed origin – primary, pseudosecondary and secondary): *a*) sample SHD-4 – light-brown crystal core, bulk inclusions of irregular shape and non-crystallographic faces, probably *P*; *b*) sample SHD-2 – light green-brown cleiophane, prismatic inclusions with traces of growth striation (“steps”) (*PS*); *c*) two inclusions in a slide from cleiophane, sample SHD-3: Vacuole of irregular shape (“*palaeolith*”) and another inclusion, probably interstitial (*P*); *d*) sample SHD-2, cleiophane: elongated flat inclusions of irregular shape (*S*); *e*) sample GYU-12a – two inclusions in different slides: interstitial (left) (*P*), and a flat inclusion in a health crack, probably *S* (right); *f*) sample GYU-12a, slide, including three phases: sphalerite and quartz (most likely synchronous), and galena (late); an oval, pseudotriangular single inclusion near to quartz (~0.5 mm) is considered *P*, another inclusion of irregular shape is quartz hosted; *g*) sample KED-8 – cluster of elongated, tubular inclusions of parallel orientation, situated just on the diffuse border between light-brown and brown bands of the crystal, probably on a growth plane, most likely *P*; *h*) sample KED-8 – a population of high- T_h inclusions on a growth plane, most likely *P*; no vapor-gas bubble is observed in some of them (arrows); *i*) sample KED-10 – short-prismatic, parallel orientated, probably on a growth plane; some of them contain trapped solids (*PS*?); *j*) sample KED-8 – single bulk inclusion of tetrahedral habit (*P*).

examination. Registration of the homogenization temperature (T_h) and the last ice melting point (T_m) was performed on heating and freezing stages, respectively. These devices are laboratory-made, as mentioned by Kotzeva *et al.* (2011).

The heating stage was made of polished bronze, placed in a ceramic vessel of 5 cm in diameter. The heater is a flat (~1 mm) washer (disk) of mica and the resistance wire (Kanthal) is wound radially around it. A Chromel/Alumel thermocouple is soldered on the bottom of the stage; the “cold” ends of its wires are temperature maintained at 0.0 ± 0.1 °C (melting ice). The thermocouple electromotive force (e.m.f.) was continuously registered by a pen recorder. At

the inclusion homogenization, when the bubble disappears, the thermocouple circuit is short-cuttet for a moment by a push-button, which drives the pen to strike a line (scratch) from the temperature pen track to the zero (base) line. This method makes possible the registration of more than one T_h in a single run of heating a sample. The length (mm) of this straight line is converted to T_h by a graph (curve) in the co-ordinates mm (length) vs T_h . The standard curve is normalized on the melting temperature of a set of standard thermometric substances: Signotherm (E. Merck) 50, 120, and 180, and analytical grade phenolphthalein (261 °C), NaNO_3 (307 °C), and $\text{K}_2\text{Cr}_2\text{O}_7$ (398 °C). A small amount (~0.5 mg)

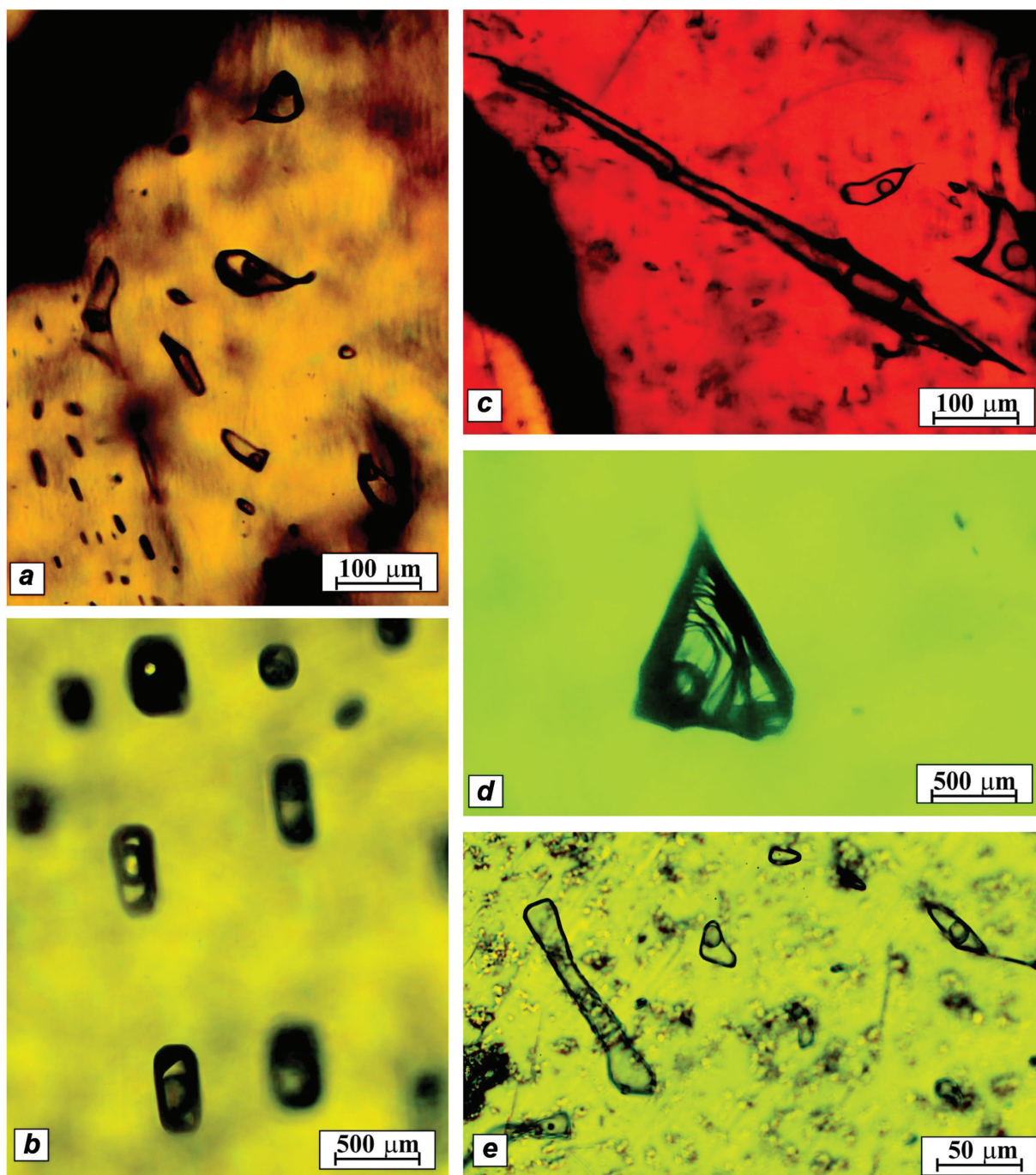


Fig. 2. Microphotographs of sphalerite-hosted fluid inclusions: *a*) sample SHD-2; *b*) sample KED-10; *c*) sample SHD-4; *d*) sample SHD-2 (Cle); *e*) sample SHD-2 (Cle). The respective temperatures of homogenization (T_h , °C) and salinities (S , wt.% NaCl-eqv.) can be found in Table 1.

of the respective substance is put between two thin (0.1 mm) glass disks of 12 mm in diameter, placed on the stage and heated to melting. The repeated measurements (5–6 runs) of T_h show the limits of the uncertainty: ± 2 °C for the temperature interval 100–200 °C and ± 3 °C for higher temperatures.

The freezing stage is an aluminium double-walled cylindrical vessel (cell) ($h = 2.5$ cm, $\varnothing_i = 5$ cm) with a glass window ($\varnothing = 12$ mm) in the centre of its bottom. A triangle stage (3 cm side) of riddled metal lamella on three legs (7 mm) is mounted on the bottom of the cell, and the slide for investiga-

tion is fixed on it by a flat spring (clip). The cell is filled with antifreeze – a mix of water, ethanol and glycerol, freezing at $-80\text{ }^{\circ}\text{C}$. A battery of three thermocouples of copper-constantan displaced under, at, and on the object supplies enough e.m.f. for measuring in mV-range.

The cells were put in an isolating styropore box; small portions of liquid nitrogen, pored in the inter-wall room, caused cooling of the object (the slide). After fluid inclusions' freeze, the liquid nitrogen flow is cut off. The slow increase in temperature with a rate of $3\text{--}1\text{ }^{\circ}\text{C}/\text{min}$ is assigned entirely to the imperfection of the thermal isolation. The signal (mV) registration is similar to the T_h determination.

As the freezing stage is laboratory-made, it needs a responsible calibration by a set of standard solutions: 0.0% (distilled water, DW), 1.0%, 3.0%, 5.0%, 9.0%, 12.0%, 15.0%, and 20.0% NaCl. The best way for preparing such solutions is weighing. For example, a 9.0% solution is made as follows: 0.900 g NaCl (analytical grade, dried at $105\text{ }^{\circ}\text{C}$) is weighed in a small vial (25 ml beaker) and DW is added up to net-weight of 10.000 g.

Small amounts (0.x mg) of these solutions are sealed in thin glass capillaries ($\varnothing \approx 0.1\text{ mm}$), 10–12 mm long. Such a sealed capillary, together with another containing DW to play a “witness”, are fixed by transparent epoxy resin between two 0.1-mm thin glass disks (12 mm in diameter). Metal or coloured glass spikes are also put in the wafer to label the salt concentration. The standard curve is built directly as e.m.f. (mV) vs salinity (% NaCl). In the range of lower concentrations, due to the nature of the cryoscopic function, the uncertainty is higher: $\pm 0.3\%$; when salinity is over 10%, it is $\pm 0.2\%$ (cf. Bodnar, 1993).

Decreptomety

The decrepitation is a relevant method for opening a bulk of inclusions. A preliminary study of this process by decreptomety may expose the relationship between decrepitation and formation of the analytical signal. Three different techniques were applied and the coincidence of the results confirms their reliability. The respective graphs (Fig. 3 – P) obtained

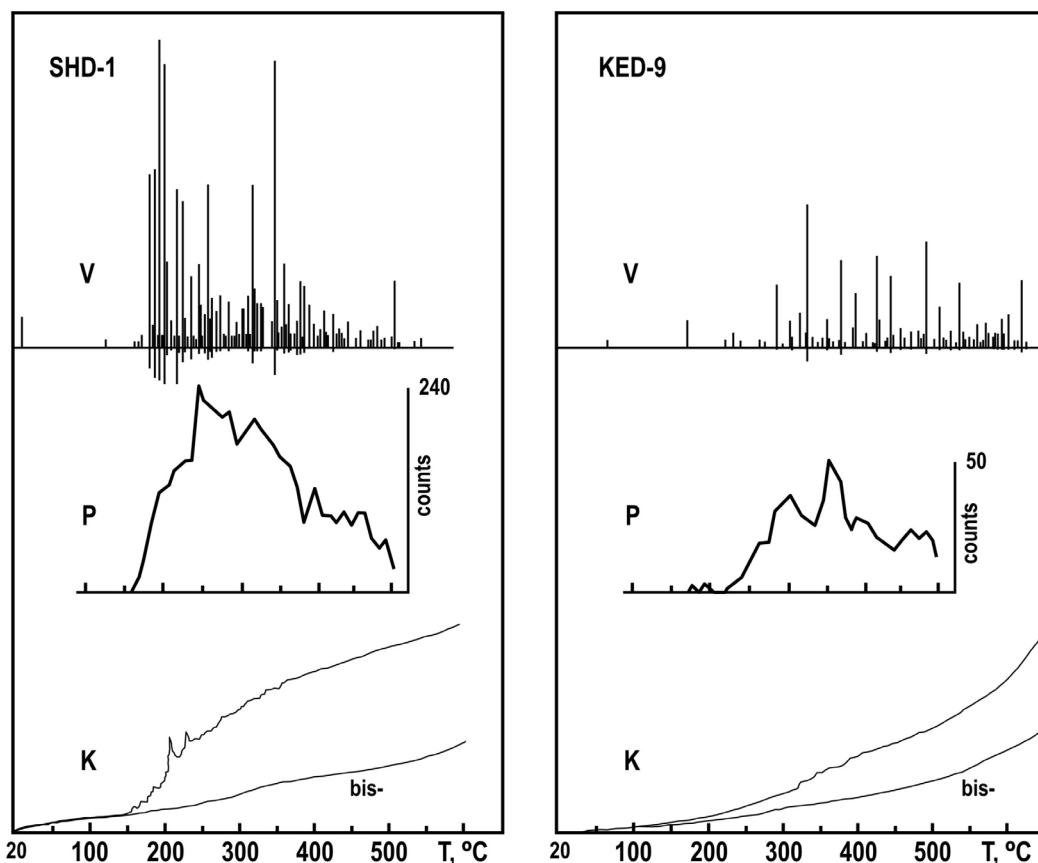


Fig. 3. Decreptomety of two sphalerite samples: SHD-1 and KED-9. V denotes vacuum decreptomety, P is for phono-, and K indicates kinetic curve. “Bis-” is the kinetic curve of already decrepitated material (sample) (i.e., a blank).

by decreptophony are kindly supplied by Ass. Prof. M. Krăsteva (cf. Dimitrov and Krăsteva, 1972). The technique of decrepitation *in vacuo* (Fig. 3 – V) and some decreptograms of fluorite and quartz are given in Piperov and Zidarova (1995) and Piperov *et al.* (2016). Mineral samples (~0.5 g grains) are subjected to kinetic study by heating them at a rate of 10 °C/min in a closed volume (~2 L) at a starting (background) pressure $p \leq 10^{-3}$ Torr. The increase in temperature activates decrepitation and, respectively, evolution of volatiles: H₂O-vapour and gases. The intensive increase in the pressure is detected by a Pirani-type manometer and recorded continuously (*e.g.*, Piperov and Zidarova, 1995) (Fig. 3 – K). This method cannot be applied to the minerals containing structural water.

Chemical analysis

D-ICP spectrometry, according to Piperov *et al.* (2016), is used for cation determination in the inclusion solute.

Analysis of the volatiles: water and gases

The decrepitation *in vacuo* by heating the sample at a high rate of 10 °C/s, but to sufficiently low temperature (just at decrepitation maximum), is known as thermo-shock. In the case of the sphalerite samples studied, $T_{\max} = 300$ °C. The aim of this strategy is reducing the amount of volatiles originating from sources other than inclusions. The sphalerite crystals are previously ground, sieved and cleaned by heating to boil in ~1 M HCl, repeatedly rinsed in DW and DDW, and dried at 80 °C.

The sphalerite sample (0.5–1.25 g, grain fraction 0.5–1.25 mm) is put into a silica-glass reactor – a part of a glass vacuum apparatus ($V \approx 200$ cm³, $p \leq 10^{-4}$ Torr). The inclusion volatiles, liberated by decrepitation, are separated in a cold trap ($T = -117$ °C: melting aether), where H₂O (vapour) freezes. A Pirani gauge traces this process and, after the total trapping of water, the dry gases are let into a mass spectrometer (MS10, AEI-Kratos). The signals are quantified by an internal standard (“tracer”): a precisely measured small amount (10–20 µl) of atmospheric Ar, containing 99.7% ⁴⁰Ar (Lanphere and Dalrymple, 1966).

The pressure of the water vapour in the isolated trap at room temperature is measured by a silicone-oil (silol) manometer. An experimentally plotted calibration curve $P_{\text{H}_2\text{O}}$ (mm silol) vs $m_{\text{H}_2\text{O}}$ (µg) is used for H₂O determination. Precisely measured amounts of water are introduced in the apparatus

for building the calibration curve. Water aliquots in the range 20–500 µg are dosed as Mg(ClO₄)₂·2H₂O (Piperov and Penchev, 1976); larger amounts (200–1000 µg) are sealed in glass capillaries, weighed on a semi-micro balance (± 0.02 mg) before and after filling with a drop of water. These micro-ampoules are broken in the vacuum apparatus and H₂O is determined as described above.

After cooling to room temperature, the reactor is opened and the decrepitated material is exposed to the air for 10–15 min, aiming at equilibrium of the surfaces, degassed on heating, with the atmosphere (H₂O, CO₂). The system is closed, evacuated and all procedures for decrepitation are repeated. The results obtained (“bis-”) are considered as a blank.

Crushing in vacuo

A suitably designed vacuum mortar is applied. It is made of stainless steel; the hemispheric bottom of the mortar (1.25 cm radius) and the pestle head are made of hard 40% Cr-steel.

A glass bell closes tightly the mortar through a Viton O-ring or by a greased ground plan-flange. The bell is supplied with two ground glass connections: the coaxial one holds vacuum-tightly a simple mechanical device to move (turn round) the pestle; another joins the mortar with the analytical (vacuum) line.

The sphalerite sample (2 g, grains) is loaded in the mortar, the glass bell is mounted, and the air is pumped out; later, the fine evacuation takes 14–15 h (overnight) by an absorption pump (activated charcoal at –195 °C (liquid nitrogen)). After closing the analytical line, the background is determined, and the data obtained are considered as a blank.

Under $p \leq 10^{-4}$ Torr, the analytical line is ready for crushing mineral grains. It proceeds through 5–10 turns of the pestle, and its efficiency is revealed in the pressure increase (Pirani-gauge). The analysis of the volatiles follows the usual path (see above).

RESULTS AND DISCUSSION

The results of the microthermometric measurements (T_h and total salinity (S), estimated based on the last ice crystal melting point), are shown in Table 1 and plotted as histograms in Fig. 4. For samples SHD-4 and SHD-6, whose material is considered identical with the sphalerite specimen studied by Bonev and Kouzmanov (2002), T_h of six fluid inclusions are found in the range 205–219 °C, whose data coincide

Table 1

A summary of the microthermometric studies (94 inclusions) and the data obtained. The inclusions of a given association (cluster), whose temperature of homogenization (T_h) and salinity (S) are equal within the uncertainty limits, are represented as a single result. The number of studied inclusions so pooled is given in the Remarks column as a multiplier ($\times n$). The assumed types of inclusions are primary (P), pseudosecondary (PS) and secondary (S). Cle = cleiophane; n.d. = not determined.

Sphalerite samples		Fluid inclusions				
Specimen ID	Relative age	Assumed type	T_h , °C	S, % NaCl-equiv.	Remarks	
SHD-1	late, Cle	PS	250	9.4	$\times 4$	
		PS	264	9.8		
		PS	247	8.5		
		PS	235	9.2		
SHD-2	late, Cle	S	156	2.8	Figs 1d, 2e	
			168	4.0		
			171	2.8		
			174	2.2		
			162	n.d.		
		PS	201	7.0		$\times 2$, Figs 1b, 2a
			205	6.7		
			213	8.4		
			222	10.0		
225	7.2	Fig. 2d				
SHD-3	late	P	n.d.	10.4	Fig. 1c	
			n.d.	10.4		
SHD-4	early, core	P	229	10.1	$\times 4$, Fig. 1a	
			232	10.4		
			239	11.0		
	late, banded periphery	PS	205	9.9	$\times 7$ (cf. Bonev and Kouzmanov, 2002)	
			209	9.1		
			212	8.9		
			210	n.d.		
			216	n.d.		
			219	n.d.		
GYU-12 GYU-12a	early	PS	254	n.d.	$\times 3$ single FI next to Qrz Qrz, Fig. 1f	
	early	P	266	6.4		
			265	7.0		
	early	P	270	6.2		
			271	6.1		
	12a	late	P	254		6.7
			S	240		5.4
	12a	early	PS	281		n.d.
			S	179		n.d.
				169		n.d.
				172		n.d.
		P	n.d.	5.4		
		PS	n.d.	7.1		
			n.d.	4.3		
KED-8	early	P	367	8.1	$\times 2$, Fig. 1h	
			370	7.6		
			366	10.9		
KED-9	early	PS	346	4.2	$\times 3$, Fig. 1g	
			346	3.0		
			346	3.8		
			341	2.8		
			341	5.1		
			344	n.d.		
			n.d.	2.8		
			n.d.	4.2		
			n.d.	3.7		
			n.d.	3.7		
KED-10	late	PS	288	5.1	$\times 2$, Fig. 1j	
			309	8.4		
			293	7.6		
			289	7.8		

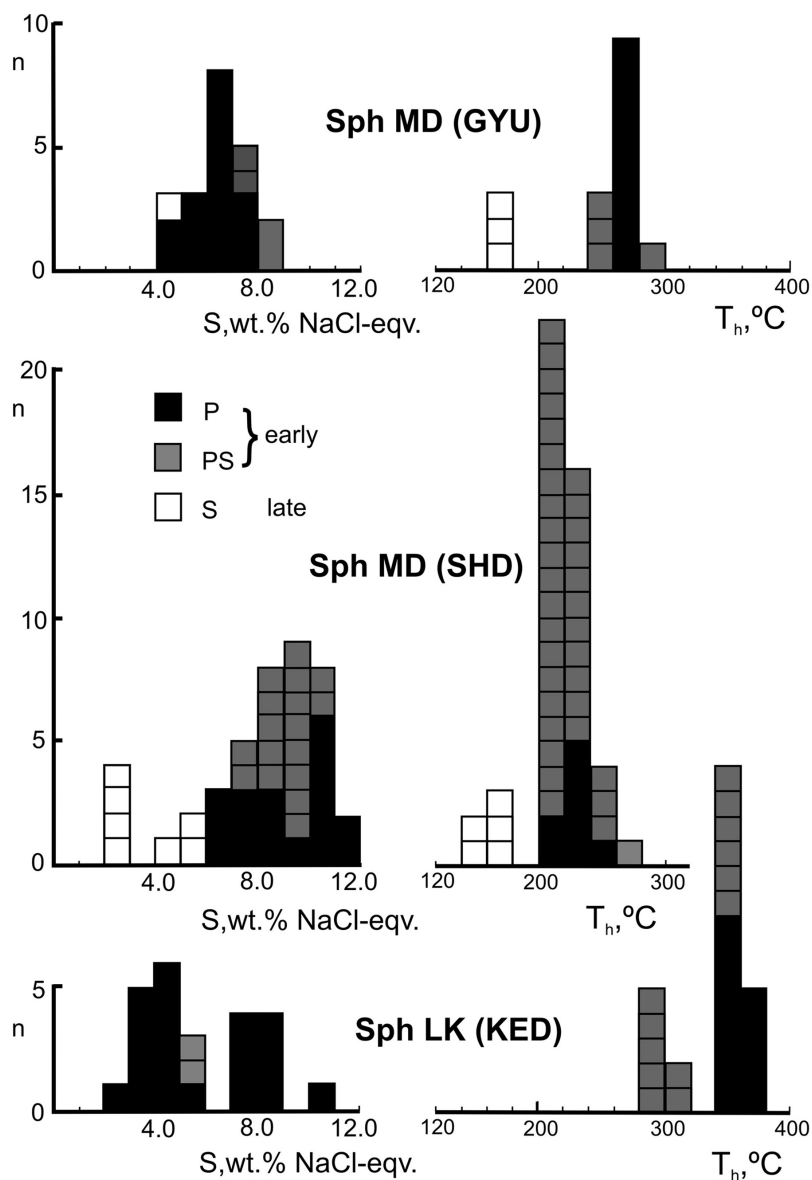


Fig. 4. Histograms of the total salinity (wt.% NaCl-equiv.) and T_h (°C) of sphalerite-hosted fluid inclusions from GYU, SHD, and KED. P, PS and S denote primary, pseudosecondary and secondary inclusions, respectively; n – number of measurements.

with the ones reported by Bonev and Kouzmanov (2002): 200–220 °C ($n = 52$). The total salinity (S) in the primary and pseudosecondary inclusions (SHD + GYU), however, is found to be high (8.9–11.0 wt.% NaCl-equiv., $n = 6$) on the background of all other determinations ($n = 20$): $S = 6.1$ – 10.4 wt.% NaCl-equiv.

From a geochemical point of view, an interrelation between homogenization temperature and the total salinity is of interest. The locations of coupled data in coordinates T_h vs S (wt.% NaCl-equiv.) for 64 inclusions are shown in Fig. 5. It is immediately evident (Figs 3, 4) that Kenan Dere sphalerites have

been deposited from solutions of higher temperature (280–374 °C), but lower salinity (2–5 wt.% NaCl-equiv.). Minčeva-Stefanova (1973) reported also $T_h = 340$ – 305 °C for Sph and $T_h = 345$ – 280 °C for Qrz. Conversely, sphalerite from Shumachevski Dol and Gyudyurska shows lower $T_h = 200$ – 230 °C, but somewhat higher salinity: $S = 6$ – 11 wt.% NaCl-equiv. Furthermore, it is likely that the KED and GYU late sphalerite was deposited at 30–50 °C lower temperatures than the earlier.

A time evolution trend of cooling and dilution of sphalerite depositing solute is illustrated also in the case of a single crystal. For specimen SHD-4, the

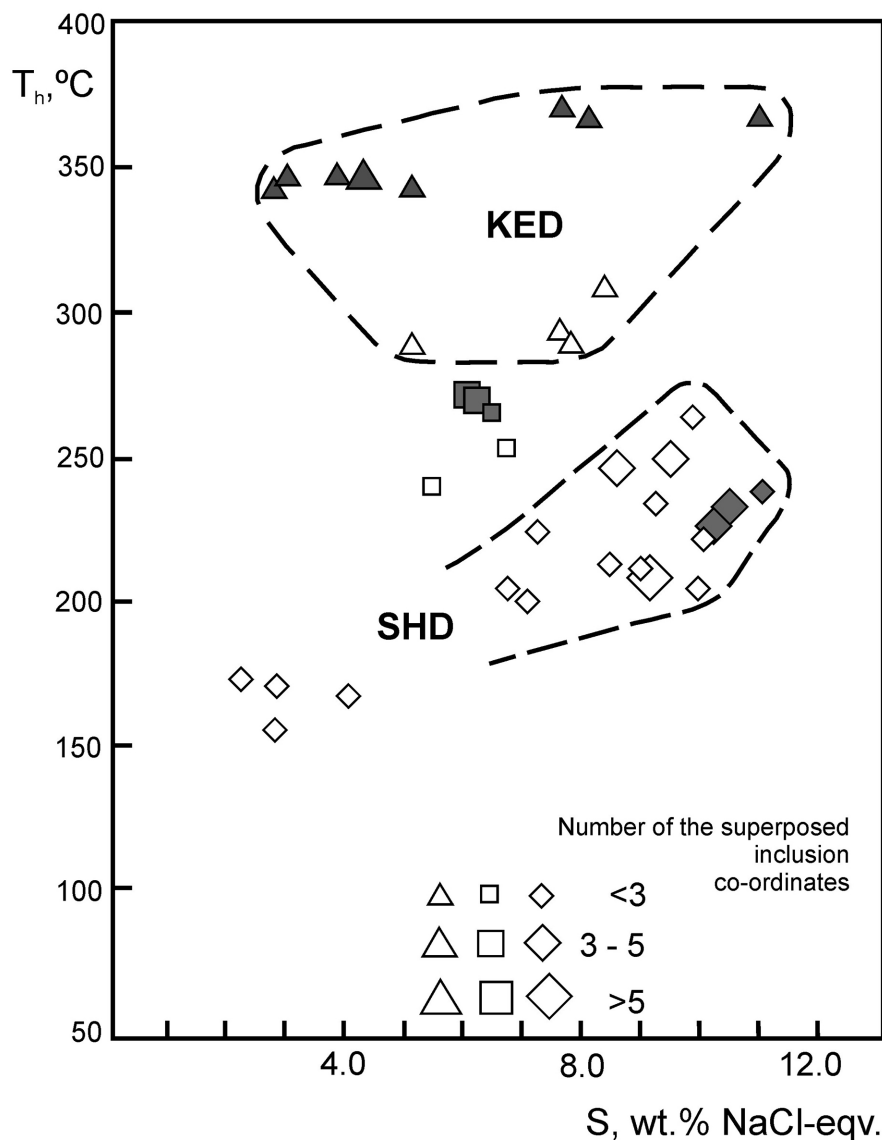


Fig. 5. Coupled data T_h (°C) vs total salinity (S , wt.% NaCl-equiv.) for 64 inclusions from SHD (diamonds), GYU (squares) and KED (triangles) deposits. The dark figures indicate early crystals or earlier parts of them; the empty figures denote later materials.

crystal core, nine inclusions show $T_h = 232 \pm 4$ °C (median) and a total salinity $S_t = 10.4 \pm 0.3$ wt.% NaCl-equiv., while for the inclusions in the crystal periphery (SHD-6, 11–12 measurements) $T_h = 204 \pm 4$ °C and $S_t = 9.1 \pm 0.3$ wt.% NaCl-equiv., respectively, were found.

The case of Kenan Dere sphalerite is of special interest. Here, three parts of a single crystal are studied again: from the core (KED-8) to the periphery (KED-10). The fluid inclusions in the two inner parts indicate a “normal” time evolution trend: a decrease in T_h from 367 ± 2 °C to 345 ± 2 °C and also a decrease in the total salinity from 8.1 ± 1.6 wt.%

NaCl-equiv to 4.0 ± 0.6 wt.% NaCl-equiv. In the other crystal part (KED-10), however, on a background of a T_h decrease to 293 ± 4 °C, the total salinity increases again up to 7.6 ± 1.2 wt.% NaCl-equiv., which admits participation of another new solution (sphalerite II?, cf. Minčeva-Stefanova, 1973).

As the analytical methods used are based on decrepitation, a more detailed preliminary investigation of this process is performed. A set of decreptograms of two sphalerite samples, SHD-1 and KED-9, are given in Fig. 3. The coincidence of the three techniques mentioned above is good, revealing their reliability. It is also worth noting that the beginning

of the intensive decrepitation of the high-temperature sample KED-9 is at higher temperature ($T > 300$ °C), while for SHD-1 decrepitation starts at $T \approx 200$ °C (see Fig. 3). The bimodal decreptogram (Fig. 3, KED-9 – P) indicates existence of fluid inclusion populations of different morphology (*e.g.*, dimensions), rather than of different generations (Kozłowski and Metz, 1989).

The chemical analysis of the principle cations is performed by D-ICP-AES. The processing of the raw data obtained from analyses of samples SHD-5 and KED-9 is presented in Table 2, 3 and all results are summarized in Table 4. Data from analyses of fluid inclusions in barren quartz from the Krushev Dol deposit, Madan district (Kotzeva *et al.*, 2011), are proposed for juxtaposition.

Unfortunately, the methods for determination of the ore element from micro-inclusions in ore host are not available. In the case of the D-ICP tech-

nique, submicro-particles from the host, obtained at explosions of near-surface inclusions, are blown by the carrier gas and introduced into the plasma, which results in a hyper-signal of the host elements. On that account, reliable data on Zn content of the inclusions in sphalerite cannot be obtained. For the brown sphalerites, Fe is also a host crystal element. Dark-coloured crystals from the deposits prospected contain up to 10.5 mol% Fe in the Madan district and up to 15.1 mol% Fe in the Laki district (Minčeva-Stefanova, 1973), showing a linear correlation between colour intensity and Fe-content. Iron may exist either as an isomorphic substitute or as solid micro-inclusions of pyrite, chalcopyrite and pyrrothite (Minčeva-Stefanova, 1973). This also refers to some other elements: Mn and Cu. Only the late sphalerite of cleiophane type from Shumachevski Dol reveal Fe/Na mmol/mol ratios (7.0 and 7.6) similar to the ones from inclusions in Qrz

Table 2
Baseline corrected and sensitivity normalized intensities (counts) from D-ISPAES analysis of sample SHD-5.

Int. No.	T°C	Na	K	Li	Cu	Mg	Fe	Al	Pb	Mn	Ca
4	126	–	–	–	–	–	–	–	–	–	–
5	171	10.3	–	–	–	–	–	–	–	–	–
6	224	55.2	–	–	–	–	–	–	–	–	–
7	275	99.9	21.1	2.0	6.2	26.8	20.9	35.3	9.2	9.6	38.9
8	326	56.6	–	–	–	–	–	–	–	–	41.6
9	377	~10	–	–	–	–	–	–	–	–	–
Σ		232	21.1	2.0	6.2	26.8	20.9	5.3	9.2	9.6	38.9
X/Na (mmol/mol)			91	8.6	27	(>100)	(90)	(>100)	(39)	(41)	(>100)

Note: Int. No. is the consecutive number of profiles (sub-integration); T°C is the temperature at the end of every sub-integration; results in brackets in all tables are considered uncertain (Piperov *et al.*, 2016) and are not processed.

Table 3
Baseline corrected and sensitivity normalized intensities (counts) from D-ISPAES analysis of sample KED-9.

Int. No.	T°C	Na	K	Li	Cu	Mg	Fe	Al	Pb	Mn	Ca
5	171	–	–	–	–	–	–	–	–	–	–
6	224	15	–	–	0.6	–	–	–	–	–	–
7	275	100	16	4.8	–	3.4	58	7.8	2.0	8	15
8	326	44	4	–	–	–	20	3.0	–	–	4
9	377	–	–	–	–	–	–	–	–	–	–
S		159	20	4.8	0.6	3.4	78	10.8	2.0	8	19
X/Na (mmol/mol)			118	28	3.6	(20)	(462)	64	12	47	(112)

Note: see note in Table 2.

Table 4
Summarized results from D-ICP-AES analyses of fluid inclusions in the sphalerites studied. $X/1000$ Na atomic ratios (mmol X/mol Na).

Deposit ID	Sample code	Remarks	X:	K	Li	Ca	Pb	$T_h, ^\circ\text{C}$ (± 10)	Chemical geothermometer, $^\circ\text{C}$		
									F&T (± 25)	Na/K (± 50)	Na/Li (± 50)
MD (SHD)	1	Cleiothane, late		110	27	66	19	250	260	277	(500)
	2	Cleiothane, late		139	(35)	44	17				
	3	Cleiothane, light-brown		84	16	65	6.1				
	4	Parts of single crystal: Light-brown core		117	19	(100)	23	247		283	(434)
	5	Brown intermediate zone		91	8.6	(>100)	(39)	232		258	(320)
	5 – bis			87	6.9	(>200)	12	232		254	(296)
6	Dark-brown periphery		100	12	82	1.8	213	255	267	(360)	
			Averages \pm SD	104 40	18 10	64 20	(17)				
MD (GYU)	12	early, black		108	10	(>100)	(>100)	260, 271		275	338
LK (KED)	8	early, light-brown core		154	26	75	<14	341, 370	290	313	(494)
	9	late, dark-brown periphery		126	30	(>100)	12	288, 301	–	291	(498)
	Qrz	D-ICP-AES (Piperov <i>et al.</i> , 2016)		94	1.6	5.8	6.6				
MD (KD)			\pm SD	30	0.5	2.0	2.0	338	300	261	(167)
	Qrz	Crush-leach ICP AES (Kotzeva <i>et al.</i> , 2011)	\pm SD	151	16	60	(>150)	338	330	311	(404)

Note: Results for Zn in inclusions are not represented, as the host is ZnS and small particles obtained during decrepitation are transported to the plasma, thus producing a hyper-signal for Zn. The chemical geothermometers used are after Fournier and Truesdell (1973) (F&T) and Verma and Santoyo (1997) (Na/K and Na/Li).

MD (KD): 8.4 and 7.9 (Piperov *et al.*, 2016). Unexpectedly, high signals of Ca, Mg and Al from three samples are assumed to be a result of (mechanical?) contamination with traces of some cryptocrystal aluminosilicate(s) (clay minerals?), insoluble in 1 M mineral acids (cf. Piperov *et al.*, 2016). On that account, the analytical results for Cu, Mg, Fe, Al and Mn are not presented in Table 4 and are excluded from discussion.

Finally, it is likely that only the results from analyses of fluid inclusions in cleiophane and partly in light-brown Sph CHD-3 (Table 4) are reliable, as well as the data for the alkaline elements. These results correspond well to the values obtained from the analyses of fluid inclusions in barren quartz from the Krushev Dol deposit (Piperov *et al.*, 2016; cf. Table 4).

An additional check on the reliance of some of the results may be done by involving these data in the chemical geothermometry. The ratios between Na, K, Ca and Li are used (Fournie and Truesdell, 1973; Verma and Santoyo, 1997); the calculated temperatures are given in Table 4, where the determined T_h is also shown. The calculated values indicate that, most likely, K/Na ratios found are close to the real one; Li/Na ratios, however, seem enhanced (20–50%).

As was mentioned above, the Zn concentration in the sphalerite-hosted fluid inclusions cannot be evaluated. For that reason, the results from analyses of fluid inclusions in syngenetic quartz offer the only possibility of obtaining information about ore elements' concentration; furthermore, all analy-

ses suggest a remarkable homogeneity of the ore-forming fluids' chemistry on a large territory in the Central Rhodope Dome (Piperov *et al.*, 1977; Bonev and Kouzmanov, 2002; Kostova *et al.*, 2004; Kotzeva *et al.*, 2011; Table 5). The differences between the mineral-forming solutions consist, first of all, in their temperature: from pericritical (370 °C) to mesothermal (200–220 °C), as well as in the total salinity: from 11.0% (~2 molar) to 2.8% NaCl-eqv. A time evolution of the solutions is perceived: from hotter and stronger in the early stages to cooler and weaker in the late one.

Kouzmanov *et al.* (2010) reported significant distinctions between ore metal concentrations in inclusions of synchronous ore and gangue minerals, whose difference suggests crystallization from different hydrothermal solutions. Fluid inclusions, however, are micro-objects, which are sealed in an environment of micro-scale, too. For example, the expected formation of an electrical double layer, up to 2–3 mm thick, may cause a local increase (of more than one log-unit) in the concentration of many ions, close to the growing crystal surface, without assumption for participation of distinct (macro-)solutions.

Finally, the present study helps us to insert successfully the Rhodope sphalerite deposition into the common knowledge of the epithermal ore formation (*e.g.*, Seward and Barnes, 1997; Borisov, 2000; Kostova *et al.*, 2004).

A summary of the inclusion fluid analyses displays that the ore-forming solute contains alkaline

Table 5

Comparison between data from fluid inclusions in sphalerite and synchronous quartz and evaluation of the Zn-concentration in the inclusions.

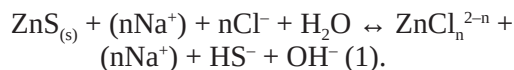
Deposit	Host	Method	Stage	Salinity %	Na (ppm) × 10 ⁴ (%)	K (ppm)	K/Na (mol)	Zn (ppm)	References
MD (YUP)	Q1	LA-ICP-MS	early	4.0	1.72	2995	0.103	10–100	Kostova <i>et al.</i> (2004)
	Q2		ore	3.7	1.28	2144	0.099	7–30	
	Q3		late	6.7	2.39	5400	0.133	10–100	
MD (KD)	Qrz	LA-ICP-MS	early	6.0	2.27	1050	0.027	20–50	Kotzeva <i>et al.</i> (2011)
			ore	8.5	3.21	5400	0.099	50–130	
			late	4.5	1.77	4200	0.140	< 45	
MD (SHD)	Sph	D-ISP-AES	early	10.4	[3.5]		N.D.	this study: Figs 2, 3; Table 4	
			intermediate	9.4	[3.1]		0.100		
MD (GYU)	Sph	D-ISP-AES	late	6.9	[2.3]		0.110		
			early	6.5	[2.2]		0.108		
LK (KED)	Sph	D-ISP-AES	early	7.6	[2.5]		0.154		
			intermediate	4.2	[1.4]		0.126		

Note: Na concentrations in square brackets are not directly measured, but evaluated from salinity data assuming NaCl/KCl ≈ 10 and the concentration of the other salts is considered negligible. N.D. – not determined.

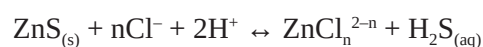
and alkaline-earth chlorides with mol ratio Na:K:Ca \approx 10:1:0.6 at low to moderate total salinity 3.7–10.4%. The ore elements (Zn, Pb, Fe, Cu) are found to be in trace concentrations, especially Zn \approx 0.001 molal, confirming very well Seward and Barnes' (1997) conclusions for the minimal concentrations of metals in ore solutions in the case of vein Cu-Pb-Zn type ore deposits. The S-species are below the limits of detection (DL): $S_{\text{tot}} < 0.3$ ppm, *i.e.*, < 0.01 molal (Piperov *et al.*, 1977). These findings suggest that the ore elements and sulphide sulphur would be transported to the locus of deposition in (nearly) stoichiometric ratios and hint that the ore substance is formed by dissolution of already existing, dispersed in the parent rocks, primordial(?) sulphides (Giggenbach, 1997). The lack of S isotope fractionation ($\delta^{34}\text{S} = 3 \pm 2\%$; 35 samples from nine deposits (Bonnev, 1984)) suggests also autochthonous sulphur.

The zinc sulphide and especially α -ZnS = sphalerite is weakly soluble in pure water at $T = 25$ °C: $pL^{25} = 25.7$ (L – solubility product) and even at $T = 300$ °C $pL^{300} = 18.2$ (Vaughan and Craig, 1978), which means equilibrium concentrations of the order of 10^{-13} molal and 10^{-9} molal at 25 °C and 300 °C, respectively (or ~ 0.01 ppb and ~ 50 ppb). It is clear that transport capacity of such a fluid is not sufficient for rich ore deposition. The presence of chloride anions in the solution changes the environment drastically, due to complexation.

The dissolution of sphalerite in chloride-containing water solutions may be described by the following equilibrium:



It is evident that this equilibrium will be displaced to the right at high Cl^- concentration and in the presence of hydronium ions (H_3O^+) to neutralize OH^- ions produced. Additionally, the equilibrium $\text{H}_2\text{S} \leftrightarrow \text{HS}^- + \text{H}^+$ displaced to the left at $T = 300$ °C and $\text{pH} \leq 8.2$, generating $\text{H}_2\text{S}_{(\text{aq})}$. For that reason, the sphalerite dissolution-deposition is described usually by the simplified equilibrium:



This equilibrium hardly reflects the exact mechanism of the process, but evidently defines the Zn (and S) mobilization.

Barrett and Anderson (1988) show that sphalerite (as well as galena) solubility depends strongly on the pH: “a decrease in pH of one unit causes an increase in metal sulphide solubility of two log units”. Thus, at $T = 300$ °C, $\text{pH} = 4$ and $mS_{\text{red}} = 0.001$, 2 molal NaCl dissolves 10^4 ppm Zn (analytical (total) concentration), *i.e.*, ~ 1 wt.%; at $\text{pH} = 5$ – about 100 ppm. This fact emphasizes the greater transporting capacity of more acid solutions. The CO_2 content in the fluid inclusions (0.93 mol/kg H_2O (mode), cf. Table 6), dissolved as H_2CO_3 with a dissociation constant at $T = 300$ °C and $\text{pK}(\text{I})^{300} = 8.7$ (Schoonen and Barnes, 1997), defines $\text{pH} = 4.37$, which is in accordance with Barrett and Anderson's (1998) model.

Table 6
MS analyses of the volatiles from fluid inclusions in the sphalerites studied.

Sample	Sample mass (m _s) g	Method	μmol per g sample			CO ₂ /H ₂ O mol/mol	mol CO ₂ /kg H ₂ O
			CO ₂	CH ₄	H ₂ O		
SHD-1 (cleiophane)	0.7	D	0.063	0.06	3.26	0.019	1.06
SHD-6 + SHD-7	0.9	D	0.233	< LOD	11.0	0.021	1.18
	2.0	C	0.018	< LOD	1.58	0.011	0.61
KED-9 + KED-10	0.7	D	0.056	0.0011	3.33	0.017	0.93±0.3
	2.0	C	0.0022	0.0008	0.14	0.016	0.87
Qrz MD (KD) (Kotzeva, 2010)	1.0	D	0.12	N.D.	9.90	0.012	0.67
	1.0	C	0.33	0.005	1.70	0.019	1.05
Gal MD (Piperov <i>et al.</i> , 1977)						0.020	1.11

D – Decrepitation by thermal shock at 300 °C; C – Crushing *in vacuo* in a steel mortar

Note: The following molecular species are traced: H₂, CH₄, N₂, O₂, C₂₋₄H_m, CO₂ and H₂O. The MS-results for N₂, O₂, C₂₋₄H_m are always below LOD (limit of detection) and they are dropped. Results for H₂ are not included in the table, either, since H₂ is considered an artefact.

The elevated temperature is another factor stabilizing the chloridozinc complexes (Barnes, 1979). Schoonen and Barnes (1997) affirm that ZnCl_2^0 dominates (over 90%) at $T = 300\text{ }^\circ\text{C}$; Kostova *et al.* (2004) believe in another species: ZnCl_4^{2-} . The prospect of inclusions in KED sphalerite gives a good example of how the elevated temperature can preserve a great transporting capacity, even in the case of diluted solutions.

Thus, the hydrothermal solution is constituted *in situ* as a closed system at a depth of *ca* 1 km, under nearly lithostatic pressure (~ 200 bar), $T \geq 350\text{ }^\circ\text{C}$ and NaCl-dominated salt content *ca* 10%. Under these conditions, the solution with a $\text{pH} \approx 4.0\text{--}4.5$ contains ore elements (Fe, Zn, Pb) as soluble chlorido-complexes; for Zn, the total concentration may reach 1 wt.%. Sulphide-S compound under these conditions is H_2S .

The development of extensional dislocations in the west slope of the Madan Dome changes the environment substantially. Firstly, they caused depressions, where the pressure dropped to hydrostatic (*i.e.*, $P \approx 100$ bar) and the pore fluids were forced in them. The pressure in the ascending hydrothermal solution gradually falls and, under suitable P-T conditions, it boils. Boiling changes the environment at least in two directions:

1) Decrease in the temperature, which leads to displacement of the equilibrium (1) to the left, *i.e.*, to destabilization of zinc chloridocomplexes and increase in the Zn^{2+} activity. The temporal decrease in temperature may be attributed also to an influx of new portions of cold meteoric water. In any case, the dilution may cause precipitation of additional amounts of sulphides (pyrite) on the account of chlorido-complexes destroying and respective increase in the metal ions' activities (Reed and Spycher, 1984). It is worthy to note the difference in the complex stability when temperature decreases. For example, the extreme chloridozinc-complex (ZnCl^+) stability decreases about 5 log-units at cooling from $300\text{ }^\circ\text{C}$ to $100\text{ }^\circ\text{C}$ ($\log K^{300} = 6.5$, $\log K^{100} = 1.7$; Seward and Barnes, 1997); while trihydrogensulphido-complex ($\text{Zn}(\text{HS})_3^-$) stability depletes insignificantly ($\log K^{100-200} = 2.9$; Vaughan and Craig, 1979). It may be assumed that this is relevant as a

mediator in sphalerite deposition at lower temperatures: $\text{Zn}(\text{HS})_3^- \leftrightarrow \text{HS}^- + \text{H}_2\text{S}_{(\text{aq})} + \text{ZnS}_{(\text{s})}$. Vaughan and Craig (1979) report that, at lower temperature ($100\text{ }^\circ\text{C}$) and high $\text{pH} = 6.7$, $\text{Zn}(\text{HS})_3^-$ competes with ZnCl_2^0 in the Zn complexation successfully enough.

2) Degassing particularly with separation of CO_2 and, hence, an increase in pH. Kostova *et al.* (2004) evaluate a $\text{pH} = 5.2$ at sphalerite deposition. Analysing the macro-inclusions in galena (Piperov *et al.*, 1979), we measured pH of the inclusion fluid directly: $\text{pH}^{20} = 6.5$ at $T = 20\text{ }^\circ\text{C}$. When this value is referred to $T = 300\text{ }^\circ\text{C}$, it is found $\text{pH}^{300} = 5.2$ (Schoonen and Barnes, 1997, fig. A3), confirming the data of Kostova *et al.* (2004). The increase in pH helps in supplying the sulphide species needed for sphalerite deposition as the dissociation constant of H_2S depends strongly on pH: to the second degree. It may be noted lastly that ore deposition in conductive faults focuses the disseminated sulphide matter in the relative small volumes of the veins, thus making possible the formation of rich ore deposits.

CONCLUSIONS

- Some new, more precise data on the homogenization temperatures (T_h) and the total salinity (as NaCl-eqv.) of fluid inclusions in sphalerites from deposits Shumachevski Dol – Gyudyurska (Madan district) and Kenan Dere (Laky district) are proposed.

- A temporal evolution of the sphalerite-depositing hydrothermal solution is observed: from high-temperature ($370\text{--}300\text{ }^\circ\text{C}$) and moderate (6–11% NaCl-eqv., 1–2 molal) salinity (early) to mesotemperature ($250\text{--}200\text{ }^\circ\text{C}$) and low salinity (4–6 wt.%) solute (late).

- The plausible role of the hydrogensulphido-complexes in the metal sulphides' deposition is noted.

Acknowledgements

The authors are indebted to Assoc. Profs Radostina Atanassova and Rossitsa Vassileva for their very useful comments.

REFERENCES

- Barnes, H.L. 1979. Solubilities of ore minerals. In: Barnes, H.L. (Ed.), *Geochemistry of Hydrothermal Ore Deposits, Second Edition. Ch. 8*. Wiley-Interscience, New York, 404–460.
- Barrett, T.J., Anderson, G.M. 1988. The solubility of sphalerite and galena in 1–5 m NaCl solutions to $300\text{ }^\circ\text{C}$. *Geochimica et Cosmochimica Acta* 52 (4), 813–820, [https://doi.org/10.1016/0016-7037\(88\)90353-5](https://doi.org/10.1016/0016-7037(88)90353-5).

- Bodnar, R.J. 1993. Revised equation and table for determining the freezing point depression of H₂O-NaCl solutions. *Geochimica et Cosmochimica Acta* 57 (3), 683–684, [https://doi.org/10.1016/0016-7037\(93\)90378-A](https://doi.org/10.1016/0016-7037(93)90378-A).
- Bonev, I. 1977. Primary fluid inclusions in galena crystals. I. Morphology and origin. *Mineralium Deposita* 12 (1), 64–76, <https://doi.org/10.1007/BF00204505>.
- Bonev, I. 1984. Mechanisms of the hydrothermal ore deposition in the Madan lead-zinc deposits, Central Rhodopes, Bulgaria. *Proceedings of the 6th IAGOD Symposium*, Stuttgart, 69–73.
- Bonev, I.K., Kouzmanov, K. 2002. Fluid inclusions in sphalerite as negative crystals: a case study. *European Journal of Mineralogy* 14 (3), 607–620, <https://doi.org/10.1127/0935-1221/2002/0014-0607>.
- Borisov, M.V. 2000. Thermodynamic models for deposition of Pb-Zn veins. *Geokhimiya* 38, 829–851 (in Russian).
- Dimitrov, D.K., Krăsteva, M.K. 1972. Decrepitation graphs of quartz from the Madan lead and zinc deposits. *Bulletin of the Geological Institute, Series Metallic and Non-Metallic Mineral Resources* 21, 179–184 (in Bulgarian).
- Fournier, R.O., Truesdell, A.H. 1973. An empirical Na-K-Ca geothermometer for natural waters. *Geochimica et Cosmochimica Acta* 37 (5), 1255–1275, [https://doi.org/10.1016/0016-7037\(73\)90060-4](https://doi.org/10.1016/0016-7037(73)90060-4).
- Giggenbach, W.F. 1997. The origin and evolution of fluids in magmatic-hydrothermal systems. In: Barnes H.L. (Ed.), *Geochemistry of Hydrothermal Ore Deposits, Third Edition, Ch. 15*. J. Wiley & Sons, Inc., London, 737–796.
- Kostova, B., Pettke, T., Driesner, T., Petrov, P., Heinrich, C.A. 2004. LAICP-MS study of fluid inclusions in quartz from the Yuzhna Petrovitsa Deposit, Madan ore field, Bulgaria. *Schweizerische Mineralogische und Petrographische Mitteilungen* 84, 25–36.
- Kotzeva, B.G. 2010. *Chemical analysis of fluid inclusions in Bulgarian minerals*. PhD thesis, Bulgarian Academy of Sciences, Sofia, 151 pp.
- Kotzeva, B.G., Guillong, M., Stefanova, E., Piperov, N.B. 2011. LA-ICP-MS analysis of single fluid inclusions in a quartz crystal (Madan ore district, Bulgaria). *Journal of Geochemical Exploration* 108 (3), 163–175, <https://doi.org/10.1016/j.gexplo.2011.01.002>.
- Kozłowski, A., Metz, P. 1989. Comments on the decrepitation method. *ECROFI, 10th Biennial Symposium of the Royal School of Mining, Imperial College, London, Abstracts*, 59–60.
- Krăsteva, M., Gadževa, T. 1986. Gas-liquid inclusions in quartz, sphalerite, fluorite and carbonate from the deposits in Erma Reka region of Madan ore district. *Geochemistry, Mineralogy and Petrology* 22, 54–68 (in Bulgarian).
- Lanphere, M., Dalrymple, G. 1966. Simplified bulb tracer system for argon analysis. *Nature* 209, 902–903, <https://doi.org/10.1038/209902b0>.
- Minčeva-Stefanova, J. 1973. Chemical composition of sphalerite from lead-zinc deposits in Bulgaria. *Bulletin of the Geological Institute, Series Geochemistry, Mineralogy and Petrography* 22, 227–303 (in Bulgarian).
- Minčeva-Stefanova, J. 1974. On the zoning of sphalerite crystals. In: Aleksiev, E., Minčeva-Stefanova, J., Radonova, T. (Eds), *Mineral Genesis*. Geological Institute of the Bulgarian Academy of Sciences, Sofia, 171–188 (in Bulgarian).
- Minčeva-Stefanova, J. 1977. Iron-content variations on mono-generation-zonal sphalerites. *Geochemistry, Mineralogy and Petrology* 6, 20–47 (in Bulgarian).
- Minčeva-Stefanova, J., Veselinov, I. 1981. Morphology and genesis of negative crystals in sphalerite from the Kenan Dere Deposit, Central Rhodope Mountains. *Geochemistry, Mineralogy and Petrology* 14, 47–66 (in Bulgarian).
- Minčeva-Stefanova, J., Pnev, I., Kirov, G.K. 1978. Iron-free sphalerites with increasing a_0 when recrystallized in the presence of sulphur. *Geochemistry, Mineralogy and Petrology* 9, 21–38 (in Bulgarian).
- Minčeva-Stefanova, J., Platonov, A.N., Ostafijčuk, I.M., and Macjuk, S.S. 1983. Colorimetric study of sphalerites of low iron content from some Bulgarian deposits. *Geochemistry, Mineralogy and Petrology* 17, 29–40 (in Russian).
- Piperov, N.B., Penchev, N.P. 1976. A possible method for dosing of small amounts of water vapour in vacuum systems to calibrate analysers for water determination. *Comptes rendus de l'Académie bulgare des Sciences* 29 (9), 1317–1319.
- Piperov, N., Zidarova, B. 1995. Fluid inclusions in synthetic fluorite crystals – checking of analytical procedures and thermal investigations. *A priori stretched inclusions?*. *Neues Jahrbuch für Mineralogie, Monatshefte* 5, 224–240.
- Piperov, N.B., Penchev, N.P., Bonev, I.K. 1977. Primary fluid inclusions in galena crystals. II. Chemical composition of the liquid and gas phase. *Mineralium Deposita* 12 (1), 77–89, <https://doi.org/10.1007/BF00204506>.
- Piperov, N.B., Ivanova, L.P., Aleksandrova, A.N. 2016. A reappraisal of decrepitation-inductively coupled plasma spectroscopy (D-ICP) for the bulk analysis of fluid inclusions in minerals. *Analytical Methods* 8 (15), 3183–3195, <https://doi.org/10.1039/C5AY01936B>.
- Reed, M., Spycher, N. 1984. Calculation of pH and mineral equilibria in hydrothermal waters with application to geothermometry and studies of boiling and dilution. *Geochimica et Cosmochimica Acta* 48 (7), 1479–1492, [https://doi.org/10.1016/0016-7037\(84\)90404-6](https://doi.org/10.1016/0016-7037(84)90404-6).
- Schoonen, M.A., Barnes, H.L. (1997). Chemical and physical data for hydrothermal systems. In: Barnes H.L. (Ed.), *Geochemistry of Hydrothermal Ore Deposits, Third Edition*. J. Wiley & Sons, Inc., London, 937–962.
- Seward, T.M., Barnes, H.L. 1997. Metal transport by hydrothermal ore fluids. In: Barnes H.L. (Ed.), *Geochemistry of Hydrothermal Ore Deposits, Third Edition, Ch. 9*. J. Wiley & Sons, Inc., London, 435–486.
- Vaughan, D.J., Craig, J.R. 1978. *Mineral Chemistry of Metal Sulfides*. Cambridge University Press, Cambridge, 575 pp.
- Verma, S.P., Santoyo, E. 1997. New improved equations for Na/K, Na/Li and SiO₂ geothermometers by outlier detection and rejection. *Journal of Volcanology and Geothermal Research* 79 (1–2), 9–23, [https://doi.org/10.1016/S0377-0273\(97\)00024-3](https://doi.org/10.1016/S0377-0273(97)00024-3).